

Sintering behavior, phase evolution and microwave dielectric properties of thermally stable $(1-x)\text{Li}_3\text{NbO}_4-x\text{CaTiO}_3$ composite ceramic

Huanfu Zhou*, Wei Wang, Xiuli Chen, Yanbing Miao, Xiaobin Liu, Liang Fang, Fen He

Guangxi Scientific Experiment Center of Mining, Metallurgy and Environment, Key Laboratory of New Processing Technology for Nonferrous Metals and Materials, Ministry of Education, College of Materials Science and Engineering, Guilin University of Technology, Guilin 541004, China

Received 18 July 2013; received in revised form 23 July 2013; accepted 25 July 2013

Available online 2 August 2013

Abstract

Microwave dielectric ceramics with the composition of $(1-x)\text{Li}_3\text{NbO}_4-x\text{CaTiO}_3$ ($0.1 \leq x \leq 0.3$) were prepared by the solid-state reaction method. The sintering behavior, phase structure, and microwave dielectric properties of $(1-x)\text{Li}_3\text{NbO}_4-x\text{CaTiO}_3$ ceramics were investigated. The samples consisted of Li_3NbO_4 and CaTiO_3 phases, and the amount of CaTiO_3 phase increased with increasing x . The microwave dielectric properties of the sintered ceramics varied with increasing CaTiO_3 content. In particular, the temperature coefficient of resonant frequency values (τ_f) can be adjusted to near-zero. Typically, 0.15 mol CaTiO_3 added $0.85\text{Li}_3\text{NbO}_4-0.15\text{CaTiO}_3$ ceramic exhibited good microwave dielectric properties with a relative permittivity of 21.9, a $Q \times f$ value of 24,900 GHz, and a τ_f value of 5.6 ppm/°C. These results indicate that $0.85\text{Li}_3\text{NbO}_4-0.15\text{CaTiO}_3$ ceramic can be a candidate in microwave dielectric resonators.

© 2013 Elsevier Ltd and Techna Group S.r.l. All rights reserved.

Keywords: A. Sintering; B. X-ray methods; C. Dielectric properties; D. Niobates; E. Functional applications

1. Introduction

With the continuing development of mobile telecommunication technologies, there is an always interest in novel ceramics for applications as dielectric resonators (DRs) at microwave frequencies (1–20 GHz) [1–3]. The resonant frequency of a DR is determined by the overall physical dimensions of the puck, the permittivity of a material and its immediate surroundings. The key properties are high-quality factor (Q , $Q=1/\tan\delta$), high relative permittivity (ϵ_r) and near-zero temperature coefficient of resonant frequency (τ_f) [4,5]. Consequently, many efforts have focused on developing dielectric materials with high ϵ_r to realize miniaturization of the component, high $Q \times f$ (f is the measuring frequency) for frequency selectivity, and near-zero τ_f for thermal stability.

Li-based ceramics have been reported to possess good microwave dielectric properties as well as a relatively low

sintering temperature. Recently, Zhou et al. [6] reported that Li_3NbO_4 ceramic could be sintered at 930 °C and exhibited good microwave dielectric properties of $\epsilon_r=15.8$, $Q \times f=55,000$ GHz, and $\tau_f=-49$ ppm/°C. Yoon et al. [7] reported that LiNb_3O_8 could be sintered at 1075 °C and had a ϵ_r of 34, a $Q \times f$ value of 58,000 GHz, and a τ_f of -96 ppm/°C. However, large negative τ_f values restricted their further applications as resonators. Generally, there are two methods to design a material with a thermal stability: (1) the use of composite materials by mixing component materials with negative and positive τ_f values [8], such as $\text{Zn}_2\text{TiO}_4-\text{TiO}_2$ [9], $\text{Mg}_4\text{Ta}_2\text{O}_9-\text{TiO}_2$ [10] and $\text{LiNb}_3\text{O}_8-\text{TiO}_2$ [7], and (2) formation of solid solutions, such as complex perovskites [11] and other systems [12,13]. CaTiO_3 exhibited a high ϵ_r of 162 and a large positive τ_f value of +859 ppm/°C [14]. Hence, we consider that the τ_f of Li_3NbO_4 ceramic may be adjusted to zero and the ϵ_r can be enhanced by adding CaTiO_3 . In this study, preparation, phase evolution, and microwave dielectric properties of $(1-x)\text{Li}_3\text{NbO}_4-x\text{CaTiO}_3$ ceramics have been investigated.

*Corresponding author. Tel.: +86 7 735 893 395; fax: +86 7 735 893 220.

E-mail address: zhouhuanfu@163.com (H. Zhou).

2. Experimental procedure

Specimens of the $(1-x)\text{Li}_3\text{NbO}_4-x\text{CaTiO}_3$ ($0.1 \leq x \leq 0.3$) ceramics were prepared by a two-step solid state reaction method. Li_3NbO_4 and CaTiO_3 compounds were synthesized by the conventional mixed-oxide route from the high-purity raw powders ($\geq 99.9\%$) of Li_2CO_3 , Nb_2O_5 , CaCO_3 , and TiO_2 . The calcining temperatures of Li_3NbO_4 and CaTiO_3 compounds are 800 and 1000 °C, respectively. The stoichiometric proportions $[(1-x)\text{Li}_3\text{NbO}_4-x\text{CaTiO}_3]$ of the above calcined powders were mixed in alcohol medium using zirconia balls for 4 h. After drying, a 5 wt% poly(vinyl alcohol) (PVA) solution was added to the powders and the resulting mixture was pressed into disks of 12 mm in diameter and ~ 6 mm in thickness at a uniaxial pressure of about 200 MPa. The samples were then heat-treated at 550 °C for 4 h to eliminate PVA, followed by sintering at 950–1050 °C for 4 h in air at a heating rate of 5 °C/min.

The crystal structure of the samples was investigated by X-ray diffraction measurement (XRD; PANalytical X'Pert PRO, $\text{CuK}\alpha 1$, 1.54059 Å). The surface micrographs of the samples were examined by scanning electron microscope (SEM; JEOL JSM6380-LV). The bulk density of the sintered samples was measured by the Archimedes method. Microwave dielectric properties were measured by the TE_{018} shielded cavity method using a network analyzer (Agilent N5230A) and a temperature chamber (Delta 9039).

The temperature coefficients of resonant frequency τ_f values were calculated using the following formula:

$$\tau_f = \frac{f_T - f_0}{f_0(T - T_0)} \quad (1)$$

where f_T and f_0 are the resonant frequencies at the measuring temperature T (85 °C) and T_0 (25 °C), respectively.

3. Results and discussion

Fig. 1 shows the X-ray diffraction (XRD) patterns of $(1-x)\text{Li}_3\text{NbO}_4-x\text{CaTiO}_3$ ceramics sintered at 1025 °C for 4 h. Besides the Li_3NbO_4 phase (PDF no. 16-0459), the CaTiO_3 phase (PDF no. 08-0091) was observed. With increasing x , the

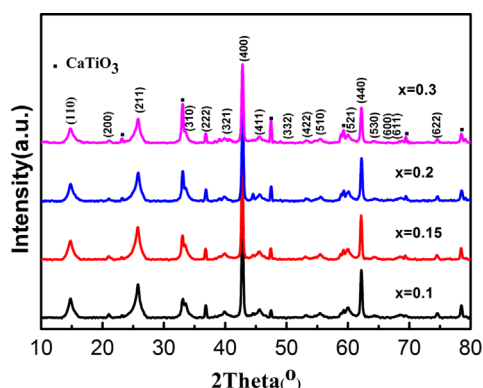


Fig. 1. XRD profiles of $(1-x)\text{Li}_3\text{NbO}_4-x\text{CaTiO}_3$ ceramics sintered at 1025 °C for 4 h.

intensity of the reflections of the Li_3NbO_4 phase decreased and that of CaTiO_3 phase increased. Both perovskite CaTiO_3 phase and cubic Li_3NbO_4 phase were presented in the $(1-x)\text{Li}_3\text{NbO}_4-x\text{CaTiO}_3$ specimens, which indicates that the temperature coefficients of resonant frequency (τ_f) of $(1-x)\text{Li}_3\text{NbO}_4-x\text{CaTiO}_3$ ceramics can be adjusted to zero by controlling the molar proportion of the Li_3NbO_4 and CaTiO_3 phases.

Fig. 2 illustrates SEM images of $(1-x)\text{Li}_3\text{NbO}_4-x\text{CaTiO}_3$ ceramics sintered at their optimized temperatures. The ceramic sintered at 950 °C contained many pores and the grain size was not uniformity. The grain size appreciably increased with increasing sintering temperature, which is attributed to higher sintering temperature (~ 1400 °C) of the CaTiO_3 phase [14]. The ceramics showed highly dense microstructure after sintering at 1025 °C. When the sintering temperature increased to 1050 °C, the grain size grew rapidly. In particular, the CaTiO_3 phase was observed, which agrees well with the results of XRD analysis. Fig. 3 shows the result from Energy-dispersive spectroscopy (EDS) of the $0.85\text{Li}_3\text{NbO}_4-0.15\text{CaTiO}_3$ ceramic sintered at 1025 °C. It can be seen that the atomic ratio between Ca and Ti is 3.52:3.67, which is near to 1:1. This result conformed that the secondary phase is CaTiO_3 phase. Hence, the result is consistent with the analysis of the XRD results.

Fig. 4 shows the bulk densities of $(1-x)\text{Li}_3\text{NbO}_4-x\text{CaTiO}_3$ ceramics sintered at different temperatures as a function of x . The bulk density increased as the sintering temperature increased from 950 °C to 1025 °C, which is attributed to the higher crystallographic calculated density ($\rho = 4.03 \text{ g/cm}^3$) of the CaTiO_3 phase. Especially, the bulk densities obviously increased when x was 0.15. However, the bulk density decreased slightly when the sintering temperature exceeded 1025 °C and even sharply decreased from 975 °C to 1000 °C ($x = 0.1, 0.2$). The decrease of the density over 1025 °C was caused by over-sintering. Due to the impurity and porosity, the bulk density of samples ($x = 0.1, 0.2$) decreased as the sintering temperature increased from 975 °C to 1000 °C.

Fig. 5 shows the relative permittivities (ϵ_r) of $(1-x)\text{Li}_3\text{NbO}_4-x\text{CaTiO}_3$ ceramics as a function of the sintering temperature. The ϵ_r increased with increasing x . The increase of ϵ_r can be explained by the higher permittivity (162) of the CaTiO_3 phase. The maximum value of ϵ_r shifted to higher temperature with increasing x , which might result from the higher sintering temperature (~ 1400 °C) of the CaTiO_3 phase [14]. Fig. 6 shows the temperature coefficients of resonant frequency (τ_f) values of the $(1-x)\text{Li}_3\text{NbO}_4-x\text{CaTiO}_3$ ceramics as a function of the sintering temperature. The τ_f values increased with increasing x , which is attributed to the higher τ_f value (+859 ppm/°C) of the perovskite CaTiO_3 phase. When $x = 0.15$, the τ_f value was tailored to near-zero (5.6 ppm/°C). Fig. 7 shows the $Q \times f$ values of $(1-x)\text{Li}_3\text{NbO}_4-x\text{CaTiO}_3$ ceramics as a function of the sintering temperature. The $Q \times f$ value increased with increasing the sintering temperature from 950 °C to 1025 °C, which is attributed to the higher sintering temperature (~ 1400 °C) of the CaTiO_3 phase and the

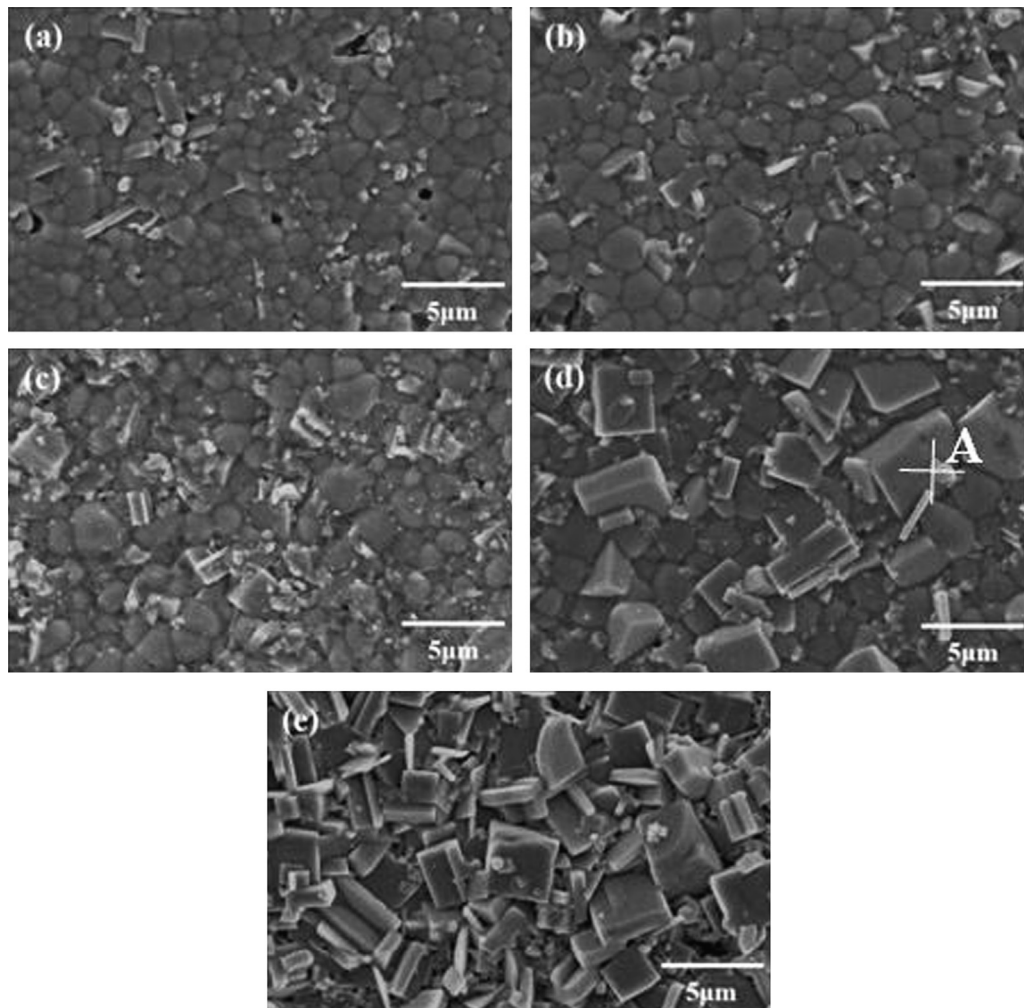


Fig. 2. SEM images of $(1-x)\text{Li}_3\text{NbO}_4-x\text{CaTiO}_3$ ($x=0.15$) ceramics sintered at different temperature: (a) 950 °C, (b) 975 °C, (c) 1000 °C, (d) 1025 °C, and (e) 1050 °C.

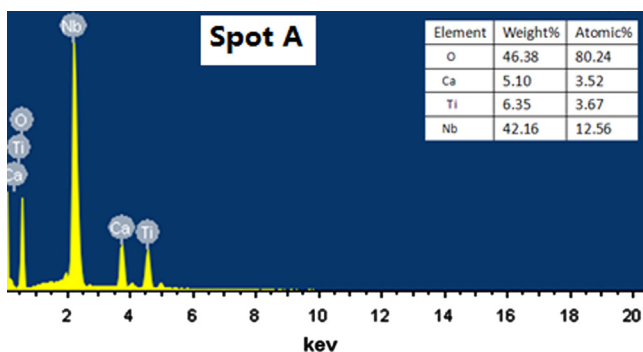


Fig. 3. EDS spectra obtained from Fig. 2(d) of $0.85\text{Li}_3\text{NbO}_4-0.15\text{CaTiO}_3$ ceramic sintered at 1025 °C.

increased bulk density with increasing the sintering temperature from 950 °C to 1025 °C. Generally, microwave dielectric loss included two parts: intrinsic losses and extrinsic losses. Intrinsic losses were caused by absorptions of phonon oscillation and extrinsic losses were caused by lattice defects. The lattice defects included impurity, cavity, substitution, size and shapes of grains, second phase, pores, etc. [15,16] The $Q \times f$

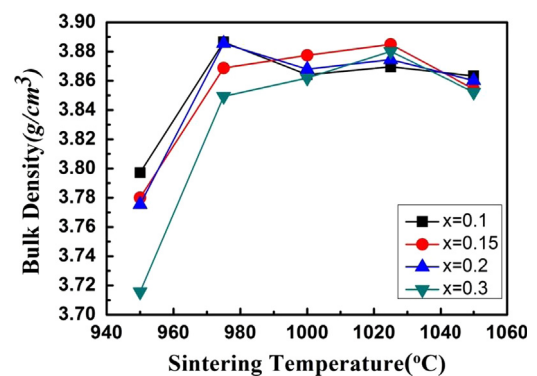


Fig. 4. Bulk densities of $(1-x)\text{Li}_3\text{NbO}_4-x\text{CaTiO}_3$ ceramics as a function of sintering temperature.

values decreased with increasing x from 0.15 to 0.3, which can be explained to the produce of the CaTiO_3 phase. When the sintering temperature is 1025 °C, the abnormal change of $Q \times f$ values in the range of $0.1 \leq x \leq 0.15$ was observed.

Due to the large negative τ_f value ($-49 \text{ ppm}/^\circ\text{C}$) of Li_3NbO_4 ceramic, perovskite CaTiO_3 ($\tau_f=+859 \text{ ppm}/^\circ\text{C}$) was

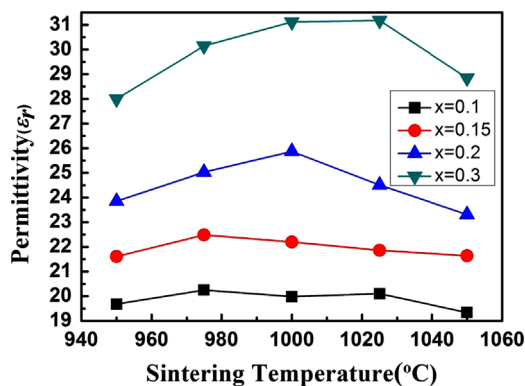


Fig. 5. Relative permittivities of $(1-x)$ $\text{Li}_3\text{NbO}_4-x\text{CaTiO}_3$ ceramics as a function of sintering temperature.

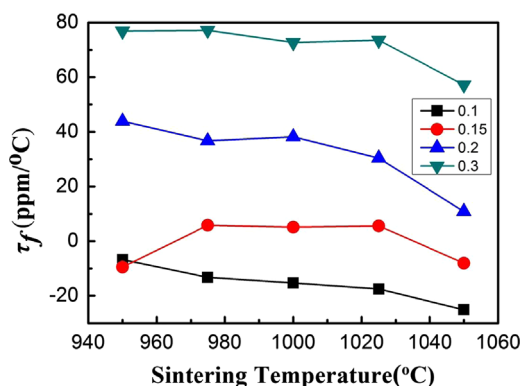


Fig. 6. τ_f values of $(1-x)$ $\text{Li}_3\text{NbO}_4-x\text{CaTiO}_3$ ceramics as a function of sintering temperature.

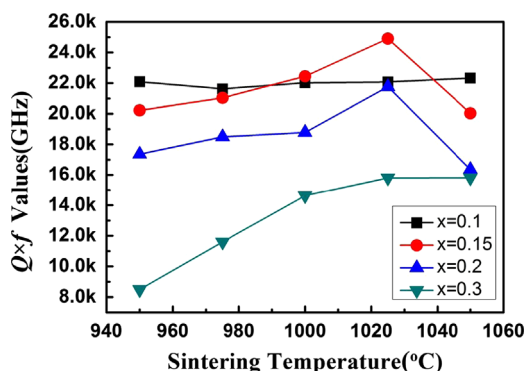


Fig. 7. $Q \times f$ values of $(1-x)$ $\text{Li}_3\text{NbO}_4-x\text{CaTiO}_3$ ceramics as a function of sintering temperature.

added to adjust the τ_f values for thermal stability. The sintering temperature, bulk density and microwave dielectric properties of $(1-x)$ $\text{Li}_3\text{NbO}_4-x\text{CaTiO}_3$ ceramics are shown in Table 1. The ϵ_r value increased from 15.8 to 31.2 and τ_f value increased from -49 ppm/°C to 73.5 ppm/°C with increasing x from 0 to 0.3. All sintered ceramics exhibited high $Q \times f$ values. In a word, the $0.85\text{Li}_3\text{NbO}_4-0.15\text{CaTiO}_3$ ceramic sintered at 1025 °C exhibited good microwave dielectric properties with a ϵ_r of 21.9, a high $Q \times f$ of 24,900 GHz, and a τ_f of 5.6 ppm/°C.

Table 1

Sintering temperature, bulk density and microwave dielectric properties of $(1-x)\text{Li}_3\text{NbO}_4-x\text{CaTiO}_3$ ceramics.

x value	ρ (g/cm ³)	Sintering temperature (°C)	ϵ_r	τ_f (ppm/°C)	$Q \times f$ (GHz)
0	3.94	930	15.8	-49	55,000
0.1	3.87	1025	20.1	-17.6	22,100
0.15	3.89	1025	21.9	5.6	24,900
0.2	3.87	1025	24.5	30.4	21,800
0.3	3.88	1025	31.2	73.5	15,800

4. Conclusion

The phase evolution, microstructure, and microwave dielectric properties of $(1-x)$ $\text{Li}_3\text{NbO}_4-x\text{CaTiO}_3$ ceramics have been investigated. The XRD analysis revealed that the Li_3NbO_4 phase can coexist with CaTiO_3 phase, and the amount of CaTiO_3 increased with increasing x . The temperature coefficients of resonant frequency (τ_f) of $(1-x)\text{Li}_3\text{NbO}_4-x\text{CaTiO}_3$ ceramics were adjusted to a near-zero value. In particular, the $0.85\text{Li}_3\text{NbO}_4-0.15\text{CaTiO}_3$ ceramic exhibits good microwave dielectric properties with a ϵ_r of 21.9, a $Q \times f$ of 24,900 GHz and a near-zero τ_f of 5.6 ppm/°C.

Acknowledgements

This work was supported by the Natural Science Foundation of China (nos. 51102058, 21261007, and 21061004), Project of Guangxi Scientific Research and Technical Development (nos. 1348020-11 and 11107006-42), Natural Science Foundation of Guangxi (nos. 2013GXNSFAA019291 and 2012GXNSFDA053024), Project of Guangxi Scientific Experiment Center of Mining, Metallurgy and Environment (no. KH2011YB019), Patent Project of Guangxi Department of Education (no. 2013ZL080), Research Start-up Funds Doctor of Guilin University of Technology (nos. 002401003281 and 002401003282), and Program to Sponsor Teams for Innovation in the Construction of Talent Highlands in Guangxi Institutions of Higher Learning.

References

- [1] T. Sebastian, *Dielectric Materials for Wireless Communications*, first Ed., Elsevier Publishers, Oxford, 2008.
- [2] H.F. Zhou, X.B. Liu, X.L. Chen, L. Fang, Y.L. Wang, $\text{ZnLi}_{2/3}\text{Ti}_{4/3}\text{O}_4$: a new low loss spinel microwave dielectric ceramic, *Journal of the European Ceramic Society* 32 (2012) 261–265.
- [3] H.F. Zhou, X.B. Liu, X.L. Chen, L. Fang, Preparation, phase structure and microwave dielectric properties of $\text{CoLi}_{2/3}\text{Ti}_{4/3}\text{O}_4$ ceramic, *Materials Research Bulletin* 47 (2012) 1278–1280.
- [4] L. Fang, D.J. Chu, H.F. Zhou, X.L. Chen, H. Zhang, B.C. Chang, C. C. Li, Y.D. Qin, X. Huang, Microwave dielectric properties of temperature stable $\text{Li}_2\text{Zn}_x\text{Co}_{1-x}\text{Ti}_3\text{O}_8$ ceramics, *Journal of Alloys and Compounds* 509 (2011) 8840–8844.
- [5] X.L. Chen, H.F. Zhou, L. Fang, X.B. Liu, Y.L. Wang, Microwave dielectric properties and its compatibility with silver electrode of $\text{Li}_2\text{MgTi}_3\text{O}_8$ ceramics, *Journal of Alloys and Compounds* 509 (2011) 5829–5832.

- [6] D. Zhou, H. Wang, L.X. Pang, X. Yao, X.G. Wu, Microwave dielectric characterization of a Li_3NbO_4 ceramic and its chemical compatibility with silver, *Journal of the American Ceramic Society* 91 (2008) 4115–4117.
- [7] S.O. Yoon, J.H. Yoon, K.S. Kim, S.H. Shim, Y.K. Pyeon, Microwave dielectric properties of LiNb_3O_8 ceramics with TiO_2 additions, *Journal of the European Ceramic Society* 26 (2006) 2031–2034.
- [8] J. Guo, D. Zhou, H. Wang, X. Yao, Microwave dielectric properties of $(1-x)\text{ZnMoO}_4-x\text{TiO}_2$ composite ceramics, *Journal of Alloys and Compounds* 509 (2011) 5863–5865.
- [9] C.F. Shih, W.M. Li, M.M. Lin, C.Y. Hsiao, K.T. Hung, Low-temperature sintered $\text{Zn}_2\text{TiO}_4\text{:TiO}_2$ with near-zero temperature coefficient of resonant frequency at microwave frequency, *Journal of Alloys and Compounds* 485 (2009) 408–412.
- [10] J.S. Kim, E.S. Choi, K.W. Ryu, S.G. Bae, Y.H. Lee, Microwave dielectric properties of $\text{Mg}_4\text{Ta}_2\text{O}_9$ ceramics with TiO_2 additions for dielectric resonator oscillator, *Materials Science and Engineering B* 162 (2009) 87–91.
- [11] Z. Liang, L.L. Yuan, J.J. Bian, Microwave dielectric characterization of the perovskite series $\text{A}_{1/2}\text{Ln}_{1/2}\text{TiO}_3\text{--NaNbO}_3$ ($\text{A}=\text{Na}, \text{Li}$; $\text{Ln}=\text{La}, \text{Nd}, \text{Sm}$), *Journal of Alloys and Compounds* 509 (2011) 1893–1896.
- [12] D. Zhou, W.G. Qu, C.A. Randall, L.X. Pang, H. Wang, X.G. Wu, J. Guo, G.Q. Zhang, L. Shui, Q.P. Wang, H.C. Liu, X. Yao, Ferroelastic phase transition compositional dependence for solid-solution $[(\text{Li}_{0.5}\text{Bi}_{0.5})_x\text{Bi}_{1-x}][\text{Mo}_x\text{V}_{1-x}]\text{O}_4$ scheelite-structured microwave dielectric ceramics, *Acta Materialia* 59 (2011) 1502–1509.
- [13] D. Zhou, H. Wang, Q.P. Wang, J. Guo, G.Q. Zhang, L. Shui, X. Yao, C. A. Randall, L.X. Pang, H.C. Liu, Microwave dielectric properties and raman spectroscopy of scheelite solid solution $[(\text{Li}_{0.5}\text{Bi}_{0.5})_{1-x}\text{Ca}_x]\text{MoO}_4$ ceramics with ultra-low sintering temperatures, *Functional Materials Letters* 3 (2010) 253–257.
- [14] V. Subramanian, V.R.K. Murthy, B. Viswanathan, Microwave dielectric properties of certain simple alkaline earth perovskite compounds as a function of tolerance factor, *Japanese Journal of Applied Physics* 36 (1997) 194–197.
- [15] S.J. Penn, N.M. Alford, A. Templeton, X. Wang, M. Xu, M. Reece, K. Schrapel, Effect of porosity and grain size on the microwave dielectric properties of sintered alumina, *Journal of the American Ceramic Society* 80 (1997) 1885–1888.
- [16] H. Tamura, Microwave Loss Quality of $(\text{Zr}_{0.8}\text{Sn}_{0.2})\text{TiO}_4$, *American Ceramic Society Bulletin* 73 (1994) 92–95.